



Synthesis and characterization of magnetic poly (acrylamide-*co*-maleic anhydride) grafted gelatin as a novel heavy metal ions wastewater treatment agent

Ning Gu, Chen Wang*, Junjie Zhang, Tingting Shen

*School of Environmental Science and Engineering, Qilu University of Technology (Shandong Academy of Sciences), Jinan 250353, China
Key Laboratory of Cleaner Production and Industrial Wastes Resourcization in Universities of Shandong, Qilu University of Technology (Shandong Academy of Sciences), Jinan 250353, China, Tel. 086-0531-89631680, email: 461897189@qq.com (N. Gu), shanqing123@126.com (C. Wang), ner8@163.com (J. Zhang), stthunanyt@163.com (T. Shen)*

Received 22 December 2017; Accepted 22 May 2018

ABSTRACT

Heavy metal pollution of water poses a severe threat to the environment and public health. In this research, a novel heavy metal ions wastewater treatment agent, magnetic (acrylamide-*co*-maleic anhydride) grafted gelatin [magnetic poly (AM-*co*-MA)-g-gelatin], was synthesized using aqueous solution polymerization. Factors affecting Cr³⁺ removal efficiency, including the amount of gelatin, Fe₃O₄ and citric acid, were optimized by orthogonal experiments to gain the optimum synthesis condition. The obtained magnetic composite was characterized by FTIR, TEM, XPS and SQUID, which showed a core/shell structure and good magnetic properties. The experimental results showed that the removal process was rapid and completed within 10 min. The residual concentration of Cr³⁺ in the solution decreased from 30 mg·L⁻¹ to 1.3 mg·L⁻¹ under the optimum condition. The magnetic composite significantly improves the removal efficiency of the Cr³⁺ by comparison with the conventional flocculants. The intensified removal performance can be due to the good magnetic separability. Therefore, the magnetic poly (AM-*co*-MA)-g-gelatin is a promising treatment agent for Cr³⁺-contaminated water.

Keywords: Heavy metal ions; Wastewater treatment agent; Magnetic composite; Synthesis; Magnetic separability

1. Introduction

With the rapid growth of industrialization, contamination of water has received extensive attention [1,2]. One major type of water contaminants is heavy metal ions [3]. In aquatic environments, they have posed a great threat to human health due to their toxicity, abundance and persistence, and they can accumulate in aquatic habitats [4,5]. There are many sources of heavy metals in the water environment, such as combustion of fossil fuels [6], leather production, electroplating production, mining and other metallurgic activities [7]. Heavy metals in industrial wastewaters include zinc, copper, cadmium, chromium [8] and

so on. Chromium is a highly toxic pollutant mainly from leather tanning, textile dyeing, electroplating [9]. In aqueous system, chromium has two main states: Cr³⁺ and Cr⁶⁺ [10]. Chromium affects human physiology health and bring about severe health problems [8]. Therefore, removing heavy metal ions from effluents is an important problem of global concern.

Up to now, a number of techniques have been developed to remove heavy metal ions from wastewater, such as adsorption, chemical precipitation, membrane filtration, ion exchange [11,12], reverse osmosis and electrochemical treatments [13]. Among these methods, chemical precipitation has attracted wide attention because of its simplicity and low cost [14]. The conventional heavy metal ions wastewater treatment agents include lime, sodium hydroxide [15], cal-

*Corresponding author.

cium sulphide, sodium sulphide [16] and so on. In addition, the application of heavy metals capturing agents has been developed such as Na₂EDTA [17], DTC [18,19]. However, the forming precipitates rely only on gravity settling to achieve the purpose of separation from water, and most of the agents show low water solubility, environmentally unfriendly [20,21] and other defects [22]. Therefore, the development of low-pollution heavy metal ions wastewater treatment agent with excellent removal efficiency and fast solid-liquid separation has been listed as an advanced research hotspot.

Nowadays, magnetic nanoparticles have been the focus of attention owing to its unique magnetic behavior [23]. They have a promising potential for various technological application such as targeted drug delivery, MR imaging [24], ferrofluids technology [25] and so on. Besides, magnetic nanoparticles are also being used for water treatment like efficient adsorption of cationic dyes [26] and separation of radionuclides [27]. In order to overcome the disadvantages of the existing chemical precipitants, a magnetic metal-organic macromolecule complex with many anionic functional groups, was prepared as heavy metal ions wastewater treatment agent. Magnetic nanoparticles is mixed with anionic polyacrylamide to form heavy metal ions wastewater treatment agent. This agent shows many excellent properties. On one hand, Fe₃O₄ has the advantage of magnetic response, which can improve the processing efficiency and shorten the action time under the synergistic effect of gravity field. On the other hand, the N atoms in the anionic polyacrylamide can form coordination bonds with metal cations, and lead to electrostatic interactions between the treatment agent and heavy metal ions. Therefore, it combines physical and chemical actions to achieve more thoroughly removal of heavy metal ions. Furthermore, the prepared magnetic composite has the advantages of no residue and no need of adjusting pH value.

The aim of the present study was to synthesize a novel heavy metal ions wastewater treatment agent, which facilitates the separation of magnetically precipitates from the aqueous solution by the application of an external magnetic field. Herein, anionic polyacrylamide was firstly synthesized and then coated onto Fe₃O₄ by aqueous solution polymerization. The synthesis conditions including monomer concentration, AM/MA mass ratio, initiator dosage and reaction time were investigated for anionic polyacrylamide's intrinsic molecular weight.

In this paper, the effects of gelatin, Fe₃O₄ and citric acid on the Cr³⁺ removal efficiency of magnetic poly (AM-co-MA)-g-gelatin were analyzed by orthogonal experimental design, and then the optimum overall performance ratio was selected. The structure, particle size, and magnetic properties of the product were characterized by FTIR, TEM, and SQUID. The most common heavy metal ion Cr³⁺, was used as the model to evaluate the removal performance of the newly prepared heavy metal ions wastewater treatment agent.

2. Experimental

2.1. Materials

All chemicals used in this study were of analytical grade, and were used without further purification. Acrylamide (AM), maleic anhydride (MA), Fe₂(SO₄)₃, FeSO₄·7H₂O were

purchased from Sinopharm Chemical Reagent Co., Ltd, Shanghai, China. Sodium bisulfite, citric acid were obtained from Nanjing Chemical Reagent Co., Ltd, Nanjing, China. Ammonium persulfate, chromium chloride, gelatin were purchased from Shanghai Macklin Biochemical Co., Ltd, Shanghai, China. Deionized water (DI) was used throughout the study.

2.2. Synthesis of poly (AM-co-MA)

Poly (AM-co-MA) was synthesized by aqueous solution polymerization which using ammonium persulfate and sodium bisulfate as redox initiator. In brief, predetermined amounts of AM and MA were put into a 250 mL three-necked flask and dissolved in 30 mL deionized water. After that a predetermined redox initiator dosage were added to the solution. Then the reaction mixture was stirred at 80°C for a period of time, followed by washing the polymer with excess amount of ethanol. The copolymer was then dried in the oven at a constant temperature of 70°C.

2.3. Measurement of intrinsic viscosity and molecular weight

A point method was used to measure the intrinsic viscosity of poly (AM-co-MA). The flow time of the solvent and the solution were measured by using Ubbelohde viscometer with capillary diameter of 0.5–0.6 mm, and the intrinsic viscosity was calculated from the measured value. The temperature was maintained at 30 ± 0.05°C during the measurement. After obtaining the intrinsic viscosity value, the molecular weight of the polymer was calculated by the following equation:

$$M = 802 [\eta]^{1.25} \quad (1)$$

where M is the molecular weight (g·mol⁻¹), $[\eta]$ is the intrinsic viscosity (mL·g⁻¹).

The parameters affecting polymerization was studied, such as monomer concentration, AM/MA mass ratio, initiator dosage and reaction time, by measure the intrinsic viscosity of poly (AM-co-MA).

2.4. Synthesis of magnetic poly (AM-co-MA)-g-gelatin

Fe₃O₄ magnetic nanoparticles was prepared by chemical co-precipitation method. The magnetic poly (AM-co-MA)-g-gelatin was synthesized by aqueous solution copolymerization method. A 250 mL three-neck flask was placed in an oil bath, 1 g of gelatin, 12.0 g of AM and 1.2 g MA were dissolved in 35 mL deionized water. In a separate beaker, 0.5 g citric acid was dissolved in 5 mL deionized water and put 2 g of Fe₃O₄ into it. Then the mixture was poured into the flask. After that, the redox initiator solution was dropwise added to the solution with stirring and the reaction mixture was stirred 90 min at 80°C. Extraction of the polymer was executed in ethanol and the copolymer was dried in the oven at a constant temperature of 40°C.

2.5. Orthogonal experimental design

The objective of orthogonal experimental design is to find an optimal production condition through a minimum

number of experiments using neatly orthogonal table. Magnetic poly (AM-co-MA)-g-gelatin specimens with different various mixture ratios were obtained by altering the amount of gelatin (factor A), the amount of Fe_3O_4 (factor B), the amount of citric acid (factor C). Amount of gelatin, Fe_3O_4 and citric acid were decided as three tests factors of orthogonal experimental and each element had three levels. It was supposed that there was no correlation between any two factors. The orthogonal matrix L_9 (3^3) was used and test procedure is given in Table 1.

2.6. Range analysis

There are two important arguments in the range analysis: k_i and R_j . k_i is defined as the average value of the total number of removal efficiency of Cr^{3+} in the equal level (i , $i = 1, 2, 3$) of each factor (j , $j = A, B, C$). The alterational trend of k_i can be used to define the optimal level. R_j represents the scope of the maximum value and minimum value of k_i . The order of R_j can be used to assess the extent that each factor affects the removal efficiency of Cr^{3+} . A larger R_j value means a greater effect on the removal efficiency [28]. For L_9 (3^3) matrix, the calculations formula are as follows (for the factor of C):

$$K1 = Y1 + Y5 + Y9 \quad (2)$$

$$K2 = Y3 + Y4 + Y8 \quad (3)$$

$$K3 = Y2 + Y6 + Y7 \quad (4)$$

$$k1 = \frac{K1}{3} \quad (5)$$

$$k2 = \frac{K2}{3} \quad (6)$$

$$k3 = \frac{K3}{3} \quad (7)$$

$$R_c = \max(k_i) - \min(k_i) \quad (8)$$

where the value of k_i is the value of factor C at i level; Y is the value of the removal efficiency of trivalent chromium in each test of orthogonal experiment. The other k values of the factor can be calculated by the same steps.

2.7. Characterizations

The functional groups of magnetic poly (AM-co-MA)-g-gelatin were distinguished by shimadzu IRA-1S WL FT-IR

Table 1
Levels and factors in orthogonal experiment design

Factors	Levels			
	Factors	1	2	3
Amount of gelatin, (g)	A	0.2	1	1.8
Amount of Fe_3O_4 , (g)	B	0.5	1	2
Amount of citric acid, (g)	C	0.2	0.5	0.8

spectra (Kyoto, Japan). Firstly, magnetic poly (AM-co-MA)-g-gelatin and KBr were mixed by triturating with mass ratio of 1:99, and then the mixture was pressed to sheet samples for FT-IR analysis. The scan wave numbers of FT-IR ranged from 500 to 4000 cm^{-1} . The size and structure of magnetic poly (AM-co-MA)-g-gelatin and Fe_3O_4 were characterized by FEI Tecnai G20 transmission electronic microscopy (TEM). The magnetic properties of magnetic poly (AM-co-MA)-g-gelatin were investigated by Superconducting Quantum Interference Device (SQUID MPMSXL), supplied by the Quantum Design Company (U.S.A.). X-ray photoelectron spectroscopy (XPS) measurements were carried out on a Thermo ESCALAB 250Xi using Al $K\alpha$ ($h\nu = 1486.6$ eV) X-ray as the excitation source for composition analysis in the precipitate.

2.8. Cr^{3+} removal experiments

The removal of Cr^{3+} (30 $\text{mg}\cdot\text{L}^{-1}$) by the magnetic poly (AM-co-MA)-g-gelatin was investigated in aqueous solution at 25°C. Then, 5 ml of poly (AM-co-MA) stock solution (1 $\text{g}\cdot\text{L}^{-1}$) was added to 200 ml Cr^{3+} aqueous solution (No. a), and 5 ml of magnetic poly (AM-co-MA)-g-gelatin stock solution (1 $\text{g}\cdot\text{L}^{-1}$) was added to 200 ml Cr^{3+} aqueous solution (No. b). They were stirred at 200 rpm for 3 min. Aftermixing, No. a was settled by gravity, No. b was placed on a magnet and settled by magnetism. The supernatant was taken and the concentration of Cr^{3+} was measured by 1,5-diphenylcarbohydrazide spectrophotometric method. Thereinto, absorbance value measurements were carried out using TU-1901 double beam UV-visible light spectrophotometer (Beijing, China) under 540 nm. The initial Cr^{3+} concentration of the solutions was controlled from 20 $\text{mg}\cdot\text{L}^{-1}$ to 1000 $\text{mg}\cdot\text{L}^{-1}$ for studying the effect of the initial Cr^{3+} concentration on the removal efficiency. All experiments were conducted in triplicate.

3. Results and discussions

3.1. Poly (AM-co-MA) of synthesis conditions optimization

Before synthesis of magnetic poly (AM-co-MA)-g-gelatin, optimization of polymerization conditions for poly (AM-co-MA) should be determined. The optimization conditions were based on the monomer concentration, AM/MA mass ratio, initiator dosage and reaction time.

3.1.1. Effect of monomer concentration on polymerization

The polymerization experiments were conducted with varying monomer concentration from 36 to 42%, whereas the concentrations of AM/MA mass ratio, initiator dosage and reaction time were kept constant at 10:1, 0.6% and 30 min, respectively. The effects of monomer concentration on intrinsic viscosity and molecular weight were researched as shown in Fig. 1A. The intrinsic viscosity and molecular weight of poly (AM-co-MA) were obviously improved with the increase of monomer concentration. At the monomer concentration of 40%, the intrinsic viscosity extended the maximum of 0.401 $\text{mL}\cdot\text{g}^{-1}$ and the molecular weight 1.905 $\times 10^6$ $\text{g}\cdot\text{mol}^{-1}$. Nevertheless, continue increased mono-

mer concentration evidently reduced the intrinsic viscosity and the molecular weight. At low monomer concentrations, free radicals and monomer can be generated fewer collision. Monomer concentration is increasing and promoting the efficiency of chain growth, which more collision happened between monomers and free radicals. Thus, a prominent increase in intrinsic viscosity and molecular weight were observed in the experiment when the monomer concentration increase from 36% to 40%. However, chain transfer and chain termination appeared under excessive monomer concentration, resulting in decreased intrinsic viscosity and molecular weight [29]. Therefore, the optimum monomer concentration accustomed in this study was 40%.

3.1.2. Effect of AM/MA mass ratio on polymerization

The effect of AM/MA mass ratio on intrinsic viscosity and molecular weight are shown in Fig. 1B. The mass ratio of AM to MA was selected as 3:1, 4:1, 5:1, 6:1, 7:1, 8:1, 9:1 and 10:1. The experiment was conducted with monomer concentration of 40%, initiator dosage of 0.6%, and reaction time of 30 min. The result indicated that intrinsic viscosity continuously increased to 400.6 mL·g⁻¹ and molecular weight increased to 1.905×10⁶ g·mol⁻¹ as the AM/MA mass ratio was increased from 3:1 to 10:1. The intrinsic viscosity is decided by the quantity of monomeric free radicals in the initiation of reaction according to the free radicals mechanism of polymerization [29]. Compared with other monomers, AM has a better reactivity ratio. With

the increase of AM dosage, the monomer polymerization rate gathered more and opportunity of collision raised between AM and main free radicals. The suitable amount of AM monomer concentration can cause chain propagation, resulting in increased intrinsic viscosity of poly (AM-co-MA). Thus, the intrinsic viscosity and molecular weight of the polymer were relatively improved. In addition, insufficient MA concentration leads to the difficulty in grafting anionic monomers to the main chain. Thus, the optimal AM/MA mass ratio of synthetic poly (AM-co-MA) was deemed to be 10:1.

3.1.3. Effect of initiator dosage on polymerization

The redox initiation system of ammonium persulfate/sodium bisulfite was used in the experiment. Fig. 1C shows the effect of initiator concentration on the intrinsic viscosity and molecular weight of the polymer, in which the monomer concentration, AM/MA mass ratio, reaction time, were 40%, 10:1, 30 min, respectively. The results were gained as the initiator dosage was changed from 0.5% to 0.8%. Results reveal that the intrinsic viscosity and molecular weight greatly increase with increased initiator dosage, but initiator dosage further increases, then decreases distinctly the intrinsic viscosity and molecular weight. In addition, the increased initiator dosage leads to the formation of primary free radicals, and anionic groups from MA are constantly grafted onto the AM which increase intrinsic viscosity and molecular weight. The maximum intrinsic

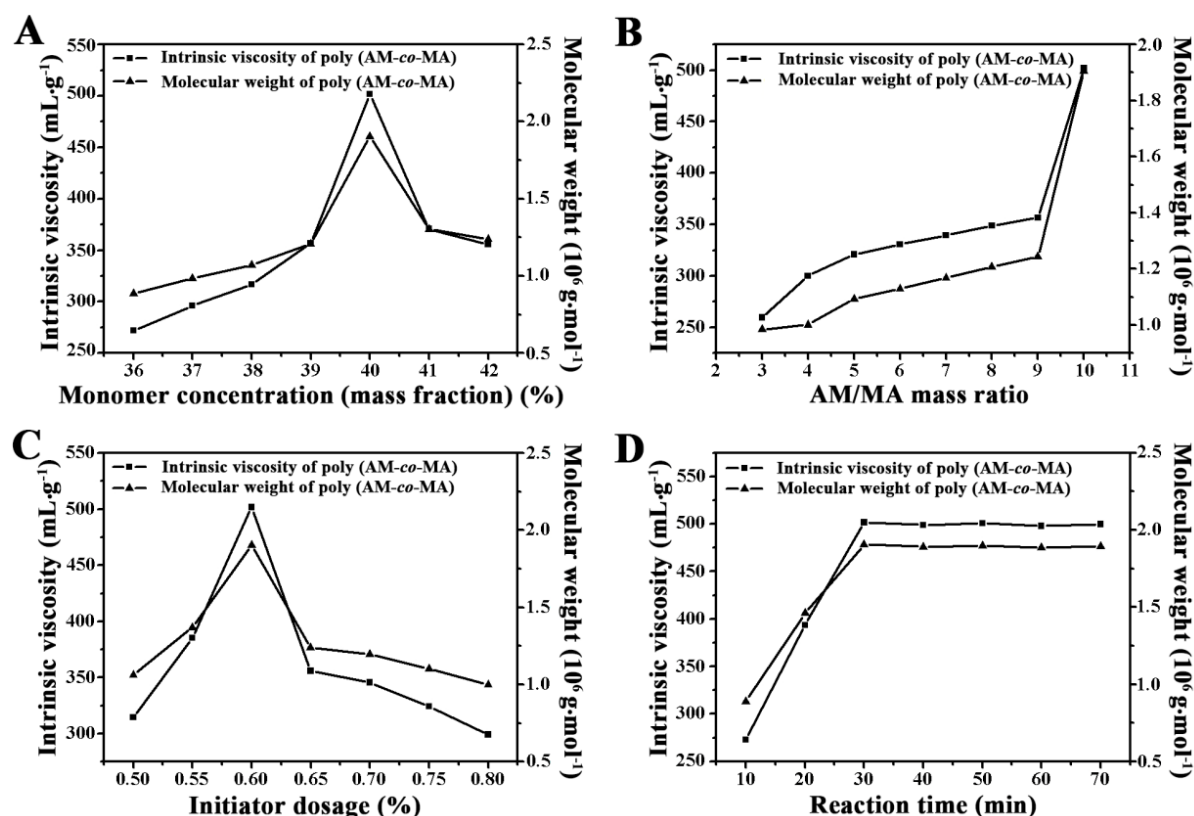


Fig. 1. Effect of monomer concentration (A), AM/MA mass ratio (B), initiator dosage (C), reaction time (D) on intrinsic viscosity and molecular weight of poly (AM-co-MA).

viscosity of 501.75 mL·g⁻¹ was obtained at initiator dosage of 0.6%. However, an obvious decrease of these two parameters was observed as the dosage was changed from 0.6% to 0.8%. A potential explanation is that too much free radicals can be generated at an excessive initiator concentration, so that a large number of active centers collide with each other. In this situation the chance of chain termination is increasing, resulting in reduction of molecular weight of poly (AM-co-MA). Accordingly, initiator dosage of 0.6% was favorable in this research.

3.1.4. Effect of reaction time on polymerization

The effect of reaction time on polymerization was appraised from Fig. 1D whereas other factors remained constant with best values. Results showed that the intrinsic viscosity and molecular weight of poly (AM-co-MA) evidently increased with the increase of reaction time and eventually remains stable after 30 min. The molecular weight of the polymer increases with reaction time. This process indicates the reaction is continuing. When the reaction time reached 30 min and continued to increase, the molecular weight of the product did not increase significantly, indicating that the polymerization reaction has been basically completed. Consequently, the best reaction time in this study was 30 min.

Basically, monomer concentration of 40%, initiator dosage of 0.6%, AM/MA mass ratio of 10:1 and reaction time of 30 min were employed for optimizing the polymerization conditions of poly (AM-co-MA). The optimized poly (AM-co-MA) was then used in subsequent preparation and characterization of magnetic poly (AM-co-MA)-g-gelatin.

3.2. Optimization strategy of orthogonal experiment

An L₉ (3³) orthogonal experiment was accomplished and the consequences are listed in Table 2. All the experiments were designed to increase the removal efficiency of Cr³⁺ by using magnetic poly (AM-co-MA)-g-gelatin.

It can be perceived that the maximum and minimum Cr³⁺ removal efficiencies of magnetic poly (AM-co-MA)-g-gelatin are 94.8% and 81.7%, respectively. Owing to the larger R_j indicates that the factor has a more significant effect on the removal rate. So among the three kinds of raw materials, the amount of Fe₃O₄ has the strongest impact on the Cr³⁺ removal efficiency, followed by the amount of gelatin, and the amount of citric acid has the weakest impact. The optimum conditions were amount of gelatin 1 g, amount of Fe₃O₄ 2 g and amount of citric acid 0.5 g.

The k value of each factor is revealed in Fig. 2. On the basis of the changes in the k value of each factor, the removal efficiency increased from 86.4% to 93.4% with the amount of Fe₃O₄ increased from 0.5 g to 2 g, suggesting that the amount of Fe₃O₄ had a significance effect on the removal rate of Cr³⁺. Meanwhile, it can be speculated that the impact of gelatin and citric acid is not obvious.

It can be speculated that the amount of Fe₃O₄ is the weightiest factor that affects the removal efficiency of Cr³⁺ by means of the orthogonal experiment and the range analysis. Magnetic poly (AM-co-MA)-g-gelatin was reprepared according to the optimum formula parameters. Thus verified the stability and dependability of the orthogonal experiment. The results showed that the Cr³⁺ removal efficiency

Table 2
L₉ (3³) orthogonal experiment list

Experimental number	Factors result (Y _i)			Cr ³⁺ removal efficiency (%)
	Amount of gelatin (g)	Amount of Fe ₃ O ₄ (g)	Amount of citric acid (g)	
1	0.2	0.5	0.2	81.7
2	0.2	1	0.8	83.9
3	0.2	2	0.5	92.1
4	1	1	0.5	92.3
5	1	2	0.2	94.8
6	1	0.5	0.8	88.9
7	1.8	2	0.8	93.2
8	1.8	0.5	0.5	88.5
9	1.8	1	0.2	90.9
K1	257.7	259.1	267.4	
K2	276	267.1	272.9	
K3	272.6	280.1	266	
k1	85.9	86.4	89.1	
k2	92.0	89.0	90.9	
k3	90.8	93.4	88.6	
Range	6.1	7	2.3	
Influence degree of factors	Fe ₃ O ₄ >Gelatin>Citric acid			
Best level	amount of gelatin 1 g amount of Fe ₃ O ₄ 2 g amount of citric acid 0.5 g			
Best group	amount of gelatin 1 g-amount of Fe ₃ O ₄ 2 g amount of citric acid 0.5 g			

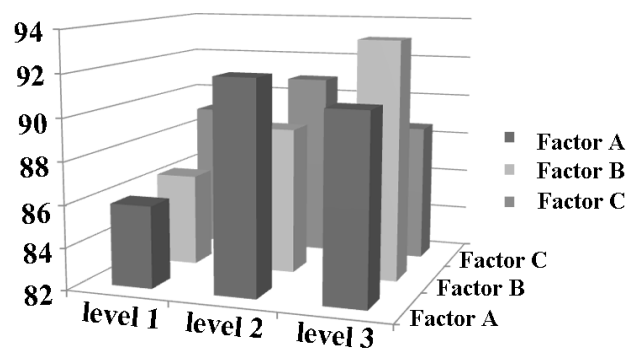


Fig. 2. Relationship between mean value of each factor and the Cr³⁺ removal efficiency.

of the magnetic poly (AM-co-MA)-g-gelatin prepared under the optimum conditions was 95.5%. The optimized magnetic poly (AM-co-MA) was then used in subsequent experiments.

3.3. Characterizations

3.3.1. Characterization of FT-IR spectrum analysis

A comparative studies on functional groups was carried out by FT-IR characterization of poly (AM-co-MA) and mag-

netic poly (AM-co-MA)-g-gelatin as shown in Fig. 3. For the spectra of magnetic poly (AM-co-MA)-g-gelatin, the characteristic absorption peaks at around 1195.0 cm^{-1} was assigned to carboxylate anion ($-\text{COO}^-$), the broad peak from 3400 cm^{-1} to 3500 cm^{-1} was observed as N-H stretching. The characteristic absorption peaks at around 1458.0 cm^{-1} and 1670.0 cm^{-1} were attributed to the stretching of C-N and C=O plane bending vibration of amide group, respectively. The peaks at 1458 cm^{-1} and 1319 cm^{-1} belonged to CH_2 scissoring and CH_2 twisting [30]. In the spectra of magnetic poly (AM-co-MA)-g-gelatin, both the absorption peaks of C-O and C=O were enhanced due to the addition of citric acid. The spectra of poly (AM-co-MA) and magnetic poly (AM-co-MA)-g-gelatin almost exhibited identical characteristic peaks. Compared with poly (AM-co-MA), the peaks assigned to Fe-O vibration at 590 cm^{-1} [31]. The results indicate that Fe_3O_4 was existed in the magnetic poly (AM-co-MA)-g-gelatin.

The analyses of the FT-IR spectra provide sufficient evidence that Fe_3O_4 was coated by the poly (AM-co-MA)-g-gelatin. During the treatment process, the precipitates rely on the synergistic effect of gravity settling and external magnetic field to achieve the purpose of separation from water, which can improve the processing efficiency and shorten the solid-liquid separation time.

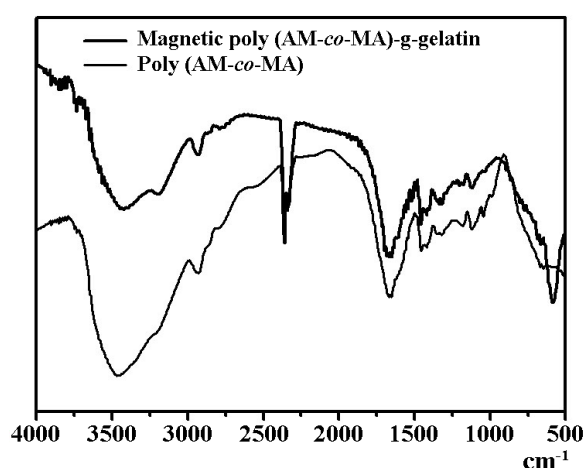


Fig. 3. FT-IR spectra of poly (AM-co-MA) and magnetic poly (AM-co-MA)-g-gelatin.

3.3.2. Characterization of TEM analysis

To give insight into shape and average size of the Fe_3O_4 magnetic nanoparticles and magnetic poly (AM-co-MA)-g-gelatin, TEM images of product are given in Fig. 4. Fig. 4A shows the representative TEM images for Fe_3O_4 magnetic nanoparticles. As can be seen from Fig. 4A, Fe_3O_4 are nearly spherical and cubic shape, having a mean diameter of about 10 nm. The TEM image of the magnetic poly (AM-co-MA)-g-gelatin prepared under the optimum conditions is shown in Fig. 4B and C. It is clear that the structure of the magnetic poly (AM-co-MA)-g-gelatin is a core-shell configuration, of which the core and the coating layer are assigned to Fe_3O_4 and poly (AM-co-MA)-g-gelatin, respectively. The shape of the magnetic poly (AM-co-MA)-g-gelatin is nearly spherical and cubic shape, which is similar to that of the Fe_3O_4 magnetic nanoparticles. The above results also indicate that the Fe_3O_4 is coated by poly (AM-co-MA)-g-gelatin, and its structure is core-shell structure.

3.3.3. Characterization of magnetic property

The characteristic of magnetism offers an easy and efficient method to separate the magnetic poly (AM-co-MA)-g-gelatin from aqueous solutions. With the help of carboxylic group, magnetic poly (AM-co-MA)-g-gelatin can be disperse in water after shaking violently and can be separated by placing a magnet on the side of the bottle as shown in Fig. 5A, indicating that magnetic poly (AM-co-MA)-g-gelatin has good dispersity and magnetic separation properties. This merit further promoted the practical use of magnetic poly (AM-co-MA)-g-gelatin in the enrichment of heavy metal ions from effluent.

Magnetization property of magnetic poly (AM-co-MA)-g-gelatin was investigated by measuring the hysteresis loop. A series of polymers with different amount of Fe_3O_4 (0.5 g, 1 g and 2 g) were prepared, and other factors remained constant with best values. The detailed synthesis methods were previously described. The amount of Fe_3O_4 were varied as 0.5 g, 1 g and 2 g, which were denoted as magnetic poly (AM-co-MA)-g-gelatin-1, magnetic poly (AM-co-MA)-g-gelatin-2 and magnetic poly (AM-co-MA)-g-gelatin-3, respectively. The magnetic hysteresis loop reveals that the magnetic poly (AM-co-MA)-g-gelatin is super paramagnetic. As shown in Fig. 5B, the saturation magnetization

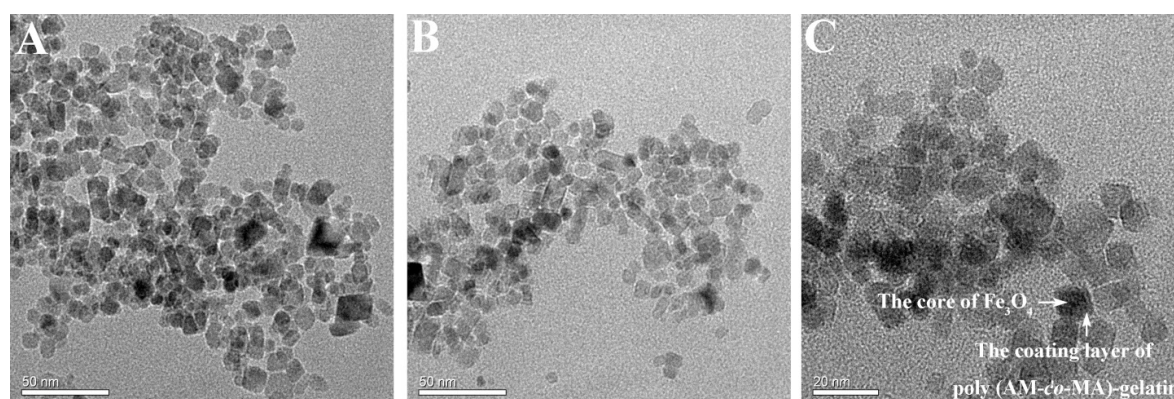


Fig. 4. TEM images of Fe_3O_4 magnetic nanoparticles (A) and magnetic poly (AM-co-MA)-g-gelatin (B, C).

value of magnetic poly (AM-co-MA)-g-gelatin-1, magnetic poly (AM-co-MA)-g-gelatin-2 and magnetic poly (AM-co-MA)-g-gelatin-3 were $15.29 \text{ emu}\cdot\text{g}^{-1}$, $26.07 \text{ emu}\cdot\text{g}^{-1}$ and $26.83 \text{ emu}\cdot\text{g}^{-1}$, respectively. The saturation magnetization value increases with rising amount of Fe_3O_4 , a possible explanation is that the magnetic response is related to the amount of Fe_3O_4 . The prominent magnetic property ensured the convenient separation in removal application.

The magnetic property analysis indicating that magnetic poly (AM-co-MA)-g-gelatin has good magnetic separation properties. Magnetic poly (AM-co-MA)-g-gelatin has

the advantage of good magnetic response, which can effectively implement rapid solid-liquid separation.

3.3.4. Characterization of XPS analysis

Surface measurements by XPS were carried out for precipitate and poly (AM-co-MA)-g-gelatin. Then the XPS spectrum was analyzed to investigate the composition of precipitate. Fig. 6 shows the XPS spectra of magnetic poly (AM-co-MA)-g-gelatin and magnetic poly (AM-co-MA)-

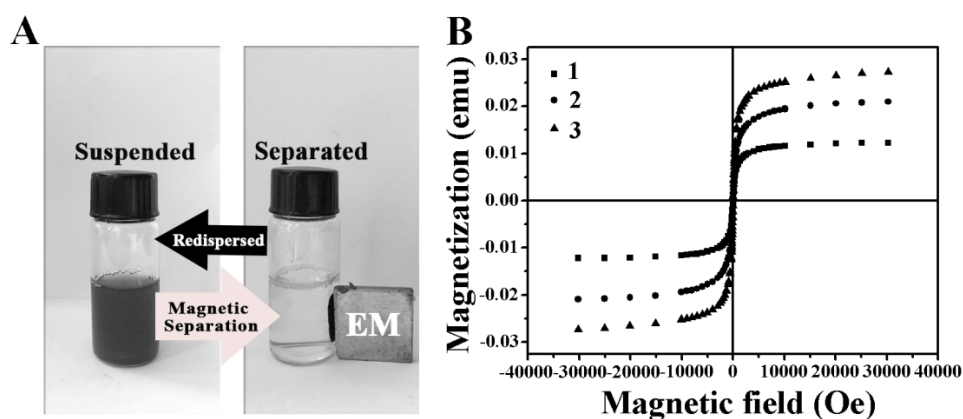


Fig. 5. Separation/redispersion property of magnetic poly (AM-co-MA)-g-gelatin under external magnetic field (A). Magnetic hysteresis loop of magnetic poly (AM-co-MA)-g-gelatin-1, 2, 3 (1, 2, 3) (B).

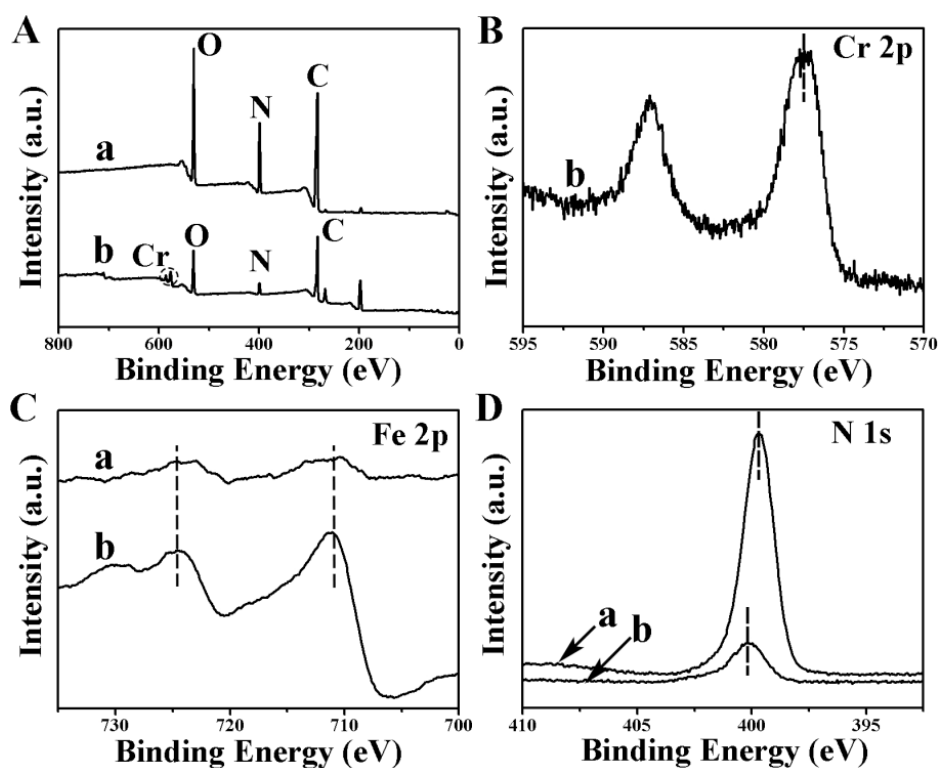


Fig. 6. Full range (A), Cr 2p (B), Fe 2p (C), N 1s (D) XPS spectra of magnetic poly (AM-co-MA)-g-gelatin (a) and magnetic poly (AM-co-MA)-g-gelatin- Cr^{3+} (b).

g-gelatin with Cr^{3+} species. After the removal process, the magnetic poly (AM-co-MA)-g-gelatin with Cr^{3+} adsorbed was gathered by magnetic separation. A typical Cr XPS peak appears in Fig. 6A after Cr adsorption. XPS of Cr 2p of magnetic poly (AM-co-MA)-g-gelatin with Cr^{3+} species (Fig. 5B) shows a peak located at 577.6 eV, and the spin orbit splitting is 9.9 ± 0.1 eV, which is typical of Cr^{3+} [32]. The results confirmed the Cr^{3+} adsorption occurred on the magnetic poly (AM-co-MA)-g-gelatin. XPS of Fe 2p of all samples (Fig. 5C) show a peak located of Fe 2p^{1/2} at 724.5 eV and Fe 2p^{3/2} at 710.4 eV, which are corresponded to the characteristic binding energies of Fe_3O_4 [33].

Fig. 6D shows the typical N 1s XPS spectra of magnetic poly (AM-co-MA)-g-gelatin before and after Cr^{3+} adsorption. Before Cr^{3+} adsorption, the peak at 399.6 eV was due to the nitrogen atoms in poly (AM-co-MA) [34]. After Cr^{3+} adsorption, however, a higher BE peak appeared in the N 1s spectrum. This was due to the magnetic poly (AM-co-MA)-g-gelatin and Cr^{3+} coordination to form a coordination complexes, in which a lone pair of electrons in the N atoms was offered to the shared bond between N and Cr^{3+} [35]. Consequently, the electron cloud density of the N atom reduces and leads to a higher BE peak observed. The XPS analysis thus provide evidence of Cr^{3+} binding to nitrogen atoms.

3.4. Removal effect of magnetic poly (AM-co-MA)-g-gelatin on Cr^{3+}

In order to assess the advantages of heavy metal ions wastewater treatment agent, the separation speed of poly (AM-co-AM) and magnetic poly (AM-co-AM)-g-gelatin were compared. The variation of the Cr^{3+} concentration as a function of time at stirring time of 3 min is shown in Fig. 7A. The initial concentration of Cr^{3+} was $30 \text{ mg}\cdot\text{L}^{-1}$. It can be seen that the Cr^{3+} content decreases sharply to $2.97 \text{ mg}\cdot\text{L}^{-1}$ within 2 min under magnetic poly (AM-co-MA)-g-gelatin treatment. When the Cr^{3+} wastewater was treated with magnetic poly (AM-co-MA)-g-gelatin, after 2, 4, 6, 8 and 10 min, the residual concentration of Cr^{3+} were 2.97, 2.46, 1.98, 1.35, $1.41 \text{ mg}\cdot\text{L}^{-1}$, respectively. After 10 min, the removal efficiency had variance insignificantly, thus the best Cr^{3+} removal efficiency can be achieved in 10 min. When the Cr^{3+} wastewater was treated with poly (AM-co-MA), the change

in Cr^{3+} concentration was not significant in 1 min and only decreased to $26.8 \text{ mg}\cdot\text{L}^{-1}$ at 10 min. These results demonstrate that the magnetic poly (AM-co-AM)-g-gelatin can remove Cr^{3+} from water in shorter settling time. This is due to the good magnetic response of magnetic poly (AM-co-MA)-g-gelatin, which is easy to separate under the effect of an external magnetic field. The magnetic poly (AM-co-AM)-g-gelatin settled rapidly after adsorbing Cr^{3+} under magnetic force, greatly reducing the processing time.

As depicted in Fig. 7B, when the initial Cr^{3+} concentration was $20 \text{ mg}\cdot\text{L}^{-1}$, Cr^{3+} removal efficiency was above 97%. The Cr^{3+} removal efficiency was reduced as the initial concentration of Cr^{3+} increased from $20 \text{ mg}\cdot\text{L}^{-1}$ to $1000 \text{ mg}\cdot\text{L}^{-1}$. However, the minimum removal efficiency in this concentration range was also higher than 90%. The anionic functional groups in the magnetic poly (AM-co-MA)-g-gelatin forms a complex with the heavy metal ions to separate the heavy metal ions from the aqueous solution under the action of magnetism. Since the existence of a certain chemical quantitative relationship between ligands and heavy metal ions, the concentration of Cr^{3+} increases will lead to reach the coordination saturation. When reaching the coordination saturation, excess Cr^{3+} can not be combined with the ligand and result in Cr^{3+} removal efficiency becomes stable.

4. Conclusions

A novel heavy metal ions wastewater treatment agent that had good magnetism was synthesized through aqueous solution polymerization method. Several parameters affecting the molecular weight of poly (AM-co-MA) were investigated. It was proved that the optimum conditions for the preparation of poly (AM-co-MA) were monomer concentration of 40%, AM/MA mass ratio of 10:1, initiator dosage of 0.6% and reaction time of 30 min. An orthogonal experiment about the determination of optimal plan with the orthogonal matrix $L_9(3^3)$ was designed, and the optimized strategy was achieved with 1g gelatin, 2 g Fe_3O_4 and 0.5 g citric acid. The as-obtained products have core/shell structure and excellent magnetic properties. The magnetic poly (AM-co-MA)-g-gelatin are very attractive for the

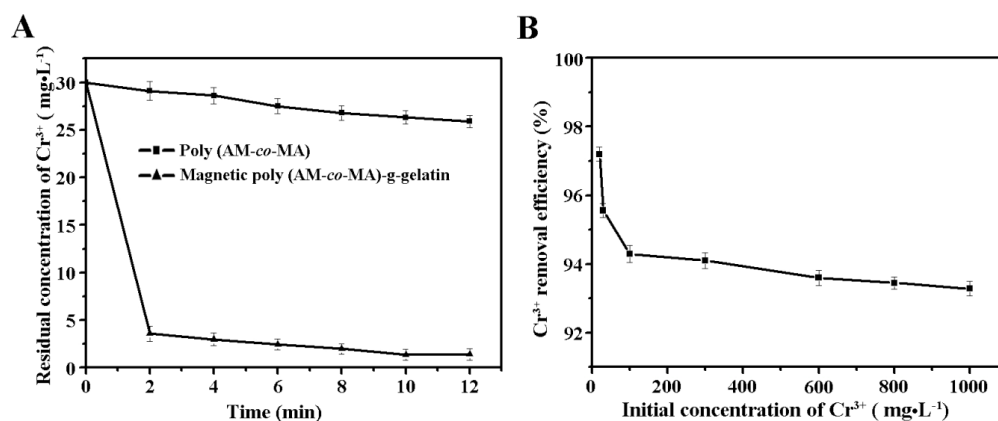


Fig. 7. Variation of the residual concentration of Cr^{3+} as a function of time (A). The effect of initial concentration of Cr^{3+} on the removal efficiency (B).

removal of Cr³⁺ because the precipitate could be easily separated from polluted water by means of a magnet.

Under the optimum condition, Cr³⁺ removal efficiency was 95.5% for simulated Cr³⁺ wastewater with initial concentration of 30 mg·L⁻¹. Compared to conventional flocculants, magnetic poly (AM-co-MA)-g-gelatin significantly increases the Cr³⁺ removal efficiency. The suggested method provides some critical advantages, including no residue, no need of adjusting pH value, as well as low Cr³⁺ concentration removal without complicated process. All these show that the prepared magnetic poly (AM-co-MA)-g-gelatin has great potential in treating Cr³⁺-contaminated water.

Acknowledgement

This project was supported by Natural Science Foundation of Shangdong Province, China (Grant No. ZR2014EEM044).

References

- [1] S.A. Nabi, A. Akhtar, Md.D.A. Khan, M.A. Khan, Synthesis, characterization and electrical conductivity of Poly-aniline-Sn(IV)tungstophosphate hybrid cation exchanger: Analytical application for removal of heavy metal ions from wastewater, *Desalination*, 340 (2014) 73–83.
- [2] M. Rawat, A.L. Ramanathan, V. Subramanian, Quantification and distribution of heavy metals from small-scale industrial areas of Kanpur city, India, *J. Hazard. Mater.*, 172 (2009) 1145–1149.
- [3] D.W. Wang, Y. Li, G.L. Puma, P. Lianos, C. Wang, P.F. Wang, Photoelectrochemical cell for simultaneous electricity generation and heavy metals recovery from wastewater, *J. Hazard. Mater.*, 323 (2017) 681–689.
- [4] N. Barlas, N. Akbulut, M. Aydogan, Assessment of heavy metal residues in the sediment and water samples of Uluabat Lake, Turkey, *Bull. Environ. Contam. Toxicol.*, 74 (2005) 286–293.
- [5] V.J.P. Vilar, C.M.S. Botelho, R.A.R. Boaventura, Copper desorption from Gelidium algal biomass, *Water Res.*, 41 (2007) 1569–1579.
- [6] E.B. Tambourgi, E.C. Muniz, A.R. Fajardo, A.T. Paulino, A.V. Reis, M.R. Guilherme, Superabsorbent hydrogel based on modified polysaccharide for removal of Pb²⁺ and Cu²⁺ from water with excellent performance, *J. Appl. Polym. Sci.*, 105 (2007) 2903–2909.
- [7] B. He, Z.J. Yun, J.B. Shi, G.B. Jiang, Research progress of heavy metal pollution in China: Sources, analytical methods, status, and toxicity, *Chin. Sci. Bull.*, 58 (2013) 134–140.
- [8] F.L. Fu, Q. Wang, Removal of heavy metal ions from wastewaters: a review, *J. Environ. Manage.*, 92 (2011) 407–418.
- [9] L. Khezami, R. Capart, Removal of chromium (VI) from aqueous solution by activated carbons: kinetic and equilibrium studies, *J. Hazard. Mater.*, 123 (2005) 223–231.
- [10] S.J. Wu, F.L. Fu, Z.H. Cheng, B. Tang, Removal of Cr(VI) from wastewater by FeOOH supported on Amberlite IR120 resin, *Desal. Water Treat.*, 57 (2016) 17767–17773.
- [11] A. Maher, M. Sadeghi, A. Moheb, Heavy metal elimination from drinking water using nanofiltration membrane technology and process optimization using response surface methodology, *Desalination*, 352 (2014) 166–173.
- [12] M. Esmat, A.A. Farghali, M.H. Khedr, I.M. El-Sherbiny, Alginate-based nanocomposites for efficient removal of heavy metal ions, *Int. J. Biol. Macromol.*, 102 (2017) 272–283.
- [13] S.H. Jang, G.Y. Jeonga, B.G. Mina, W.S. Lyoob, S.C. Lee, Preparation and lead ion removal property of hydroxyapatite/polyacrylamide composite hydrogels, *J. Hazard. Mater.*, 159 (2008) 294–299.
- [14] M.A. Hashim, S. Mukhopadhyay, J.N. Sahu, B. Sengupta, Remediation technologies for heavy metal contaminated groundwater, *J. Environ. Manage.*, 92 (2011) 2355–2388.
- [15] W.S. Zhang, C.Y. Cheng, Y. Pranolo, Investigation of methods for removal and recovery of manganese in hydrometallurgical processes, *Hydrometallurgy*, 101 (2010) 58–63.
- [16] A.E. Lewis, Review of metal sulphide precipitation, *Hydrometallurgy*, 104 (2010) 222–234.
- [17] M. Mohsen-Nia, P. Montazeri, H. Modarress, Removal of Cu²⁺ and Ni²⁺ from wastewater with a chelating agent and reverse osmosis processes, *Desalination*, 217 (2007) 276–281.
- [18] S.T. Akar, D. Arslan, T. Alp, Ammonium pyrrolidine dithiocarbamate anchored symphoricarpus albus biomass for lead(II) removal: Batch and column biosorption study, *J. Hazard. Mater.*, 227–228 (2012) 107–117.
- [19] R. Say, E. Birlik, A. Denizli, A. Ersöz, Removal of heavy metal ions by dithiocarbamate-anchored polymer/organosmectite composites, *Appl. Clay Sci.*, 31 (2006) 298–305.
- [20] Z.W. Yuan, J.M. VanBriesen, Bacterial growth yields on EDTA, NTA, and their biodegradation intermediates, *Biodegradation*, 19 (2008) 41–52.
- [21] D. Kołodyńska, The effect of the novel complexing agent in removal of heavy metal ions from waters and waste waters, *Chem. Eng. J.*, 165 (2010) 835–845.
- [22] F.L. Fu, R.M. Chen, Y. Xiong, Comparative investigation of N,N'-bis (dithiocarboxy)piperazine and diethyldithiocarbamate as precipitants for Ni(II) in simulated wastewater, *J. Hazard. Mater.*, 142 (2007) 437–442.
- [23] A.K. Singh, O.N. Srivastava, K. Singh, Shape and Size-dependent magnetic properties of Fe₃O₄ nanoparticles synthesized using piperidine, *Nanoscale. Res. Lett.*, 12 (2017) 298.
- [24] J.X. An, X.G. Zhang, Q.Q. Guo, Glycopolymer modified magnetic mesoporous silica nanoparticles for MR imaging and targeted drug delivery, *Colloids Surf., A.*, 482 (2015) 98–108.
- [25] M. Kishimoto, R. Miyamoto, T. Od, Magnetic fluid with high dispersion and heating performance using nano-sized Fe₃O₄ platelets, *J. Magn. Magn. Mater.*, 398 (2016) 200–204.
- [26] T. Yao, S. Guo, C.F. Zeng, C.Q. Wang, L.X. Zhang, Investigation on efficient adsorption of cationic dyes on porous magnetic polyacrylamide microspheres, *J. Hazard. Mater.*, 292 (2015) 90–97.
- [27] W.C. Song, M.C. Liu, R. Hu, X.L. Tan, J.X. Li, Water-soluble polyacrylamide coated-Fe₃O₄ magnetic composites for high-efficient enrichment of U(VI) from radioactive wastewater, *Chem. Eng. J.*, 246 (2014) 268–276.
- [28] X. Wu, D.Y.C. Leung, Optimization of biodiesel production from camelina oil using orthogonal experiment, *Appl. Energy*, 88 (2011) 3615–3624.
- [29] J.Y. Ma, K. Fu, J. Shi, Y.J. Sun, X.X. Zhang, L. Ding, Ultraviolet-assisted synthesis of polyacrylamide-grafted chitosan nanoparticles and flocculation performance, *Carbohydr. Polym.*, 151 (2016) 565–575.
- [30] D.R. Biswa, R.P. Singh, Characterisation of carboxymethyl cellulose and polyacrylamide graft copolymer, *Carbohydr. Polym.*, 57 (2004) 379–387.
- [31] J. Li, C.L. Chen, Y. Zhao, J. Hu, D.D. Shao, X.K. Wang, Synthesis of water-dispersible Fe₃O₄@b-cyclodextrin by plasma-induced grafting technique for pollutant treatment, *Chem. Eng. J.*, 229 (2013) 296–303.
- [32] R. Yang, Y. Wang, M. Li, Y. Hong, A new carbon/ferrous sulfide/iron composite prepared by an in-situ carbonization reduction method from hemp (*Cannabis sativa L.*) stems and its Cr (VI) removal ability, *ACS Sustain. Chem. Eng.*, 2 (2014) 1270–1279.
- [33] H. Zhu, C. Hou, Y.J. Li, G.H. Zhao, X. Liu, K. Hou, Y.F. Li, One-pot solvothermal synthesis of highly water-dispersible size-tunable functionalized magnetite nanocrystal clusters for lipase immobilization, *Chem. Asian J.*, 8 (2013) 1447–1454.
- [34] Y. Zhao, Y. Chen, M. Li, S. Zhou, A. Xue, W. Xing, Adsorption of Hg²⁺ from aqueous solution onto polyacrylamide/attapulgitite, *J. Hazard. Mater.*, 171 (2009) 640–646.
- [35] L. Jin, R. Bai, Mechanisms of lead adsorption on chitosan/PVA hydrogel beads, *Langmuir*, 18 (2002) 9765–9770.